Thermally Induced Bi(III) Lone Pair Stereoactivity: Ferroelectric Phase Transition and Semiconducting Properties of (MV)BiBr$_5$ (MV = methylviologen)

Wenhua Bi,[†] Nicolas Leblanc,[†] Nicolas Mercier,*,[†]
Pascale Auban-Senzier[‡] and Claude Pasquier[‡]

[†]*Laboratoire de Chimie et Ingénierie Moléculaire d'Angers,
UMR-CNRS 6200, Université d'Angers, Angers 49045,
France, and* [‡]*Laboratoire de Physique des Solides,
UMR-CNRS 8502, Bât. 510, Université Paris Sud,
Paris 91405, France*

Organic−inorganic hybrid systems have absorbed more and more attention of material chemists in the past decade due to the opportunity to combine distinctive properties of both components in one material. In fields of extensively studied halometalate hybrids, compounds based on Sn(II), Pb(II), Sb(III), and Bi(III) ions have demonstrated special attraction for device applications due to their electronic[1,2] or optical[3] properties as well as their room-temperature processability.[4] The inherent structural characteristic of these elements of groups 14 and 15 is their ns^2 electronic lone pair which can be more or less stereochemically active. An obvious trend is that the coordination geometry of the metal ion is a slightly distorted octahedron, revealing a rather weak lone pair stereoactivity,[5] and this trend becomes the rule when the radii of metal centers and halide atoms increase (i.e., M = Pb, Bi, X = I).[6] However, the degree of distortion of a specific MX$_6$ octahedron depends on its coordination environment and partly on the nature of organic cations also. For instance, by rationally changing the nature of cations, the inorganic networks of a series of 1D SnI$_3$ anion-based hybrids can be tuned from face-shared regular octahedra to edge-shared square-based pyramids.[7] Furthermore, the lone pair of M(II) or M(III) centers has a key role in the collective properties of materials: for instance, its stereochemical inactivity in hybrid perovskites, which are materials based on corner-shared M(II)X$_6$ octahedra, is correlated to low band gaps and improved conductivities,[1,8−10] while its stereochemical activity favors the formation of acentric materials that can display peculiar optical[3] or ferroelectric properties.[11]

Among all of the halogenometalate anions M$^{(III)}$X$_n^{(n-3)-}$ (M = Bi, Sb and X = I, Br), most of them are clusters, while 1D infinite networks, typically MX$_4^-$ and MX$_5^{2-}$, are comparatively rare.[12] The MX$_5$ chains exist as two isomers, where octahedra are either cis-connected (common) or trans-connected (rare). The trans-MX$_5$ chain, which is also known in hybrids of Pb(II) or Sn(II), can be considered as the $m = 1$ member of the ⟨110⟩-oriented hybrid perovskite family. In the [NH$_2$C(I)=NH$_2$]ASnI$_5$ system, depending on the nature of A, the trans-SnI$_5$ chain can be either regular (stereochemically inactive lone pair, A = formamidinium)[13] or adopts alternation of short and long Sn−I distances along the chain (stereochemically active lone pair, A = iodoformamidinium).[14]

In this communication, we report the synthesis, X-ray single crystal structures, and electrical and dielectric properties of (MV)BiBr$_5$, where MV^{2+} is the methylviologen dication, a well-known electron acceptor which has been frequently incorporated into salts with charge transfer property.[15] Herein, we will show that MV^{2+} stabilizes unprecedented regular BiBr$_5$ chains of trans-connected octahedra at room temperature (β-phase) and that the Bi^{3+} electronic lone pair is sterochemically activated when crystals were cooled down below −30 °C, leading to the acentric α-phase. The stereochemical activation of the lone pair is correlated with an increase of the band gap, as determined from conductivity measurements and, interestingly, with the transfer from a para- to a ferroelectric phase.

(MV)BiBr$_5$ was synthesized by solvothermal method from a mixture of BiBr$_3$, 4,4′-bipyridine, and concentrated HBr in methanol.[16] The in situ formation of MV^{2+}

(1) Takahashi, Y.; Obara, R.; Nakagawa, K.; Nakano, M.; Tokita, J.; Inabe, T. *Chem. Mater.* **2007,** *19,* 6312.
(2) (a) Mitzi, D. B.; Dimitrakopoulos, C. D.; Rosner, J.; Meideros, D. R.; Xu, Z.; Noyan, C. *Adv. Mater.* **2002,** *14,* 1772. (b) Mitzi, D. B.; Chondroudis, K.; Kagan, C. R. *IBM J. Res. Dev.* **2001,** *45*(1), 29.
(3) (a) Bi, W.; Louvain, N.; Mercier, N.; Luc, J.; Rau, I.; Kajzar, F.; Sahraoui, B. *Adv. Mater.* **2008,** *20,* 1013. (b) Mercier, N.; Barres, A. L.; Giffard, M.; Rau, I.; Kajzar, F.; Sahraoui, B. *Angew. Chem.* **2006,** *45,* 2100. (c) Guloy, A. M.; Tang, Z.; Mirana, B.; Srdanov, V. I. *Adv. Mater.* **2001,** *13,* 833.
(4) (a) Mitzi, D. B. *J. Mater. Chem.* **2004,** *15,* 2355. (b) Mitzi, D. B. *Chem. Mater.* **2001,** *13,* 3283.
(5) Fisher, G. A.; Norman, N. C. *Adv. Inorg. Chem.* **1994,** *41,* 233.
(6) (a) Wheeler, R. A.; Kumar, P. N. V. *J. Am. Chem. Soc.* **1992,** *114,* 4776. (b) Atanasov, M.; Reinen, D. *J. Am. Chem. Soc.* **2002,** *124,* 6693.
(7) Lode, C.; Krautscheild, H. *Z. Anorg. Allg. Chem.* **2001,** *627,* 841.
(8) Sourisseau, S.; Louvain, N.; Bi, W.; Mercier, N.; Rondeau, D.; Boucher, F.; Buzaré, J. Y.; Legein, C. *Chem. Mater.* **2007,** *19,* 600.
(9) Mitzi, D. B. *Chem. Mater.* **1996,** *8,* 791.
(10) (a) Mitzi, D. B.; Feild, C. A.; Schlesinger, Z.; Laibowitz, R. B. *J. Solid. State Chem.* **1995,** *114,* 159. (b) Thiele, G.; Serr, B. *Z. Kristallogr.* **1996,** *211,* 48.
(11) (a) Szklarz, P.; Galazka, M.; Zielinski, P.; Bator, G. *Phys. Rev. B* **2006,** *74,* 184111. (b) Jakubas, R.; Piecha, A.; Pietraszko, A.; Bator, G. *Phys. Rev. B* **2005,** *72,* 104107. (c) Jakubas, R.; Krzewska, U.; Bator, G.; Sobczyk, L. *Ferroelectrics* **1988,** *77,* 129.
(12) Mercier, N.; Louvain, N.; Bi, W. *CrystEngComm* **2009,** *11,* 720.
(13) Mitzi, D. B.; Liang, K.; Wang, S. *Inorg. Chem.* **1998,** *37,* 321.
(14) Wang, S.; Mitzi, D. B.; Field, C. A.; Guloy, A. *J. Am. Chem. Soc.* **1995,** *117,* 5297.
(15) Recent papers: (a) Zhang, Q.; Wu, T.; Bu, X.; Tran, T.; Feng, P. *Chem. Mater.* **2008,** *20,* 4170. (b) Ju, Z.-F.; Yao, Q.-X.; Zhang, J. *Dalton Trans.* **2008,** 355. (c) Xu, G.; Guo, G.; Wang, M.; Zhang, Z.; Chen, W.; Huang, J. *Angew. Chem., Int. Ed.* **2007,** *46,* 3249. (d) Yoshikawa, H.; Nishikiori, S. *Dalton Trans.* **2005,** 3056.
(16) A Teflon-lined PARR autoclave was heated in a programmable oven with the following parameters: 2 h heating from 25 to 120 °C, 2 h remaining at 120 °C, and then 12 h cooling down to 25 °C. Dark red crystals were collected by filtration and washed with cold ethylacetate (yield 70−80% on the basis of BiBr$_3$).
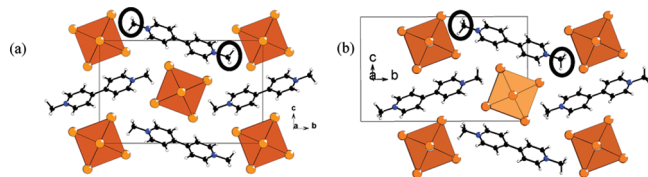
Figure 1. General view along the chains of the room temperature (β-phase (a)), and the low temperature (α-phase (b)) structures of (MV)BiBr$_5$. Circles highlight the two methyl groups of methylviologen dications which are in staggered (a) or eclipsed (b) conformations.

dications, which has been already reported,[17] can be explained by the reaction of 4,4′-bipyridine and methyliodide (also in situ formed by the reaction of methanol and HI). The deep red crystals of β-(MV)BiBr$_5$ undergoes a phase transition when the sample was cooled down to -30 °C. This process is followed by X-ray powder thermodiffractometry studies and is proved to be reversible (Supporting Information). X-ray single crystal diffraction experiments are performed on the same single crystal at room temperature and at -40 °C to determine the structures of both phases.

Both structures crystallize in the monoclinic crystal system: the β-phase (RT) was refined in the space group $P2_1/c$ and the α-phase in $P2_1$, respectively.[18] Both structures can be described as BiBr$_5$ chains separated by planar methylviologen dications, which define a chessboard arrangement when viewed along the chains (Figure 1). Remarkably, while almost all of the other 1D MX$_5$ (M = Bi, Sb; X = I, Br) networks form chains being built from cis-connected octahedra, the BiBr$_5$ chain in (MV)BiBr$_5$ adopt the trans-connected mode. To our best knowledge, only one compound with such trans-connected octahedra chains has been reported so far (bromoantimonate salt),[19] and the SbBr$_6$ octahedra in chains are heavily distorted. In contrast, in β-(MV)BiBr$_5$, unprecedented BiBr$_5$ regular chains built from nearly regular BiBr$_6$ octahedra (d(Bi$-$Br$_{axial}$): 2 × 2.926(1) Å, d(Bi$-$Br$_{equatorial}$): 2 × 2.826(1) Å and 2 × 2.849(1) Å, Br$-$Bi$-$Br bond angles of 180° and ranging from 87.92(3)° to 92.08°(3)) are stabilized. This structural feature can be partly related to the special dication of methylviologen MV^{2+} which, as
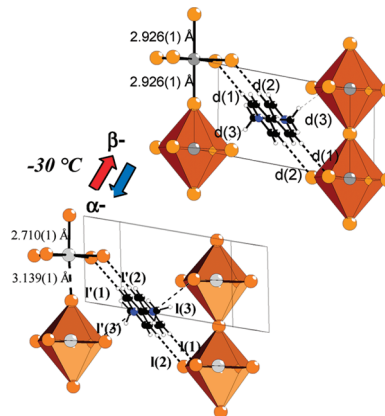

Figure 2. Part of α- and β-structures of (MV)BiBr$_5$ showing weak interactions between one methylviologen dication (see text for d(1), d(2), l(1), ...), and two BiBr$_5$ chains, and the coordination geometry of Bi^{3+}.

an electron acceptor entity, can slightly modify the charge density at the organic$-$inorganic interface, then affording new halometalate networks such as the PbI$_3$ and Bi$_2$Cl$_8$ 1D anions found in (MV)(PbI$_3$)$_2$[20] and (MV)Bi$_2$Cl$_8$,[15c] respectively.

The phase transfer from β to α is not accompanied by any distinct change of unit cell parameters since the maximum relative decrease is only 0.4% for the c axis (β: 10.372(2) Å, α: 10.318(2) Å). However, two structural features are noticeable. The first one concerns the two methyl groups of the methylviologen dications: they are staggered (by looking along the molecular axis) in the β-phase as a result of the central symmetry, while they are eclipsed in the α-phase (see circles in Figure 1). The other obvious feature is a collective effect which is a sliding of axial bromides toward bismuth atoms along the chain axis, leading to an alternation of short ($d = 2.710(1)$ Å) and long ($d = 3.139(1)$ Å) Bi$-$Br$_{axial}$ bond distances along the a axis and finally to polar chains (Figure 2). The geometry of the Bi^{3+} center is a distorted octahedron, the distances of four Bi$-$Br$_{equatorial}$ bonds being comparable to those found in the β-phase (2.818(3) Å, 2.821(2) Å, 2.838(3) Å, and 2.873(3) Å), while the angles of cis or trans Br$-$Bi$-$Br bonds range from 85.30(6)° to 92.17(6)° and from 176.01(2)° to 177.38(6)°, respectively. As already mentioned, such distorted octahedron reveals the Bi(III) lone pair stereoactivity, and we notice that the geometrical characteristics of BiBr$_6$ polyhedra (one strong, one weak, and four intermediate bonds) are well corresponding to one of the configurations described in the Brown's model,[21] indicating that the lone pair orbital extends along the direction opposite to the short Bi$-$Br bond. The overall structure of α-(MV)BiBr$_5$ is then based on polar inorganic chains running along the a axis, the polarity of symmetry (2_1axis)-related chains along the $(b + c)$ direction being approximately opposite (Figure 1). The methylviologen dications are embedded between polymeric anions in such a way that (aromatic) H$\cdots$Br contacts and N$^+\cdots$Br interactions occur in the molecular

(17) Hou, J.-J.; Guo, C.-H.; Zhang, X.-M. *Inorg. Chim. Acta* **1996**, *359*, 39.

(18) X-ray diffraction data of selected single crystals were collected on a Bruker-Nonius KAPPA-CDD diffractometer equipped with a graphite-monochromated Mo Kα radiation (λ = 0.71073 Å). Structures were solved and refined using the Shelxl97 package. Positions and atomic displacement parameters were refined by full-matrix least-squares routines against F^2. All hydrogen atoms were treated with a riding model. Crystal data for β-: C$_{12}$H$_{14}$BiBr$_5$N$_2$, M = 794.78, monoclinic, $P2_1/c$, a = 5.851(1) Å, b = 16.252(3) Å, c = 10.372(2) Å, β = 100.77(2)°, V = 968.9(3) Å^3, Z = 2, T = 293(2) K, $R_{(F)}$ = 0.041 (2391 ind. reflections, R(int) = 0.051, 96 parameters), $wR2_{(F2)}$ = 0.086 (all data), GOF = 1.15, max/min residual electron density 1.56/$-$1.64 e Å^{-3}. Crystal data for α-: C$_{12}$H$_{14}$BiBr$_5$N$_2$, M = 794.78, monoclinic, $P2_1$, a = 5.845(1) Å, b = 16.248(3) Å, c = 10.318(2) Å, β = 101.12(3)°, V = 961.5(3) Å^3, Z = 2, T = 233(2)K, $R_{(F)}$ = 0.042 (5089 ind. reflections, R(int) = 0.041, 184 parameters), $wR2_{(F2)}$ = 0.085 (all data), GOF = 1.12, Flack parameter: 0.50(2), max/min residual electron density 1.31/$-$1.90 e Å^{-3}.

(19) Carola, J. M.; Freedman, D. D.; McLaughlin, K. L.; Reim, P. C.; Schmidt, W. J.; Hass, R. G.; Broome, W. J.; DeCarlo, E. A.; Lawton, S. L. *Cryst. Struct. Commun.* **1976**, *5*, 393.

(20) Tang, Z.; Guloy, A. M. *J. Am. Chem. Soc.* **1999**, *121*, 452.
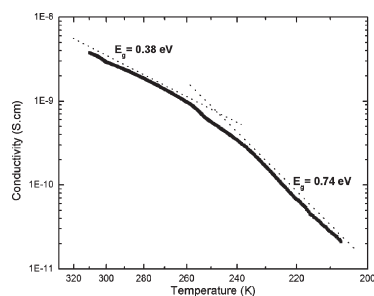
(21) Brown, D. J. *J. Solid State Chem.* **1974**, *11*, 214.

Figure 3. Conductivity of a single crystal of (MV)BiBr$_5$ as a function of the inverse of the temperature. Dotted lines represent the fits of the data by an Arrhenius law (ln $\propto E_g/2k_BT$) shifted from the data for clarity.
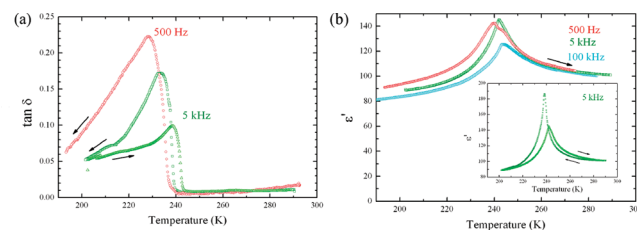

Figure 4. Dielectric losses (a) and dielectric constant (b) as a function of temperature for different applied frequencies. The arrows indicate the evolution of the temperature (heating or cooling) during the experiment. Inset: thermal cycling of the dielectric constant at a fixed frequency.

plane and perpendicular to it, respectively (Figure 2). While H$\cdots$Br distances are equal in both structures ($d(1) \simeq l(1) \simeq l'(1) \simeq 2.78$ Å, $d(2) \simeq l(2) \simeq l'(2) \simeq 2.85$ Å) and comparable to those reported in the literature,[22] the N$\cdots$Br distance varies slightly from β to α (β: $d(3)$ 3.600(1) Å; α: $l(3)$ 3.568(2) Å, $l'(3)$ 3.548(2) Å). Other weak H$\cdots$Br contacts are observed, especially those engaging the activated H atoms of methyl groups.

A correlation between the band gap or the conductivity of hybrids and the lone pair stereochemical activity of Pb(II) or Sn(II) has been already established from series of hybrid perovskite structures, either (R)MI$_4$[1,23] or (R)MI$_3$[24] incorporating different kinds of organic cations (R). Here, the only (MV)BiBr$_5$ hybrid offers us the opportunity to clearly observe the impact of the Bi(III) lone pair on its electrical behavior, especially through the transition. The conductivity of a single crystal of (MV)BiBr$_5$ as a function of the inverse of the temperature is shown in Figure 3. The conductivity is extracted from the conductance by assuming that the current flows in the full thickness of the sample. In this respect, the measured value, which is quite low, as expected in such system, must be nevertheless considered as a minimum value. The noticeable feature is that the band gap deduced from the conductivity versus temperature curve presents a strong change at -25 ± 5 °C correlated with the α- to β-phase transition determined from X-ray diffraction experiments. The increase of the band gap of 0.36 eV (from 0.38 to 0.74 eV), as the electronic lone pair becomes stereochemically active, is in good accordance with behaviors in Pb(II) or Sn(II) hybrids where the band gaps of compounds based on octahedral MX$_6$ entities are smaller than those based on distorted octahedral MX$_6$ entities.[1,23,24] It must be also noted that the calculated band gap is much smaller than the optical gap extracted from UV$-$vis spectroscopy (see SI) which is about 2 eV at ambient temperature and consistent

with the red color of the samples. This difference can be attributed to two different possibilities: the first one is the presence of defects in the sample leading to impurity levels in the band gap. The second possibility is that the measured gap is the difference between the LUMO of the organic part and the HOMO of the inorganic part. Anyway, we can anticipate from previous results of electronic structure calculations of such hybrids that the increasing of the band gap in α is correlated to a weak disperse (HOMO) band along the chain direction.[8,23]

The transition from the high temperature β-phase to the low temperature α-phase is accompanied by a loss of the symmetry center of the lattice leading to a possible ferroelectric transition. Figure 4 shows both the dielectric losses (tan δ) and the dielectric constant (ε') as a function of temperature for different frequencies. All the characteristic features for a clear ferroelectric transition at about -30 °C are present, that is, a peak in ε' correlated to a divergence of tan δ at the same temperature. As shown in the inset, a weak thermal hysteresis is observed in the real part of the dielectric constant which is associated to possible inhomogeneities in the sample leading to a possible finite range of transition temperatures. This is confirmed by the weak shrinking of the dielectric peak upon increasing frequency.

In conclusion, MV^{2+} cations have stabilized unprecedented regular BiBr$_5$ chains of trans-connected octahedra. Interestingly, the Bi^{3+} electronic lone pair is stereochemically activated below -30 °C, leading to an acentric polar phase. This is correlated with an increase of the band gap and with a para- to a ferroelectric phase transition. Polarization measurements to characterize the ferroelectric nature of the α-phase, as well as syntheses of other potential solution processing ferroelectric (MV)MX$_5$ materials (M = Sb^{III}, Bi^{III}, X = Cl, Br, I), are in progress.

Supporting Information Available: Crystallographic data as CIF files and XRPD in the -60 °C RT range and UV$-$vis spectrum (PDF). This material is available free of charge via the Internet at http://pubs.acs.org.

(22) (a) Habib, H. A.; Hoffman, A.; Höppe, H. A.; Steinfeld, G.; Janiak, C. *Inorg. Chem.* **2009**, *48*, 2166. (b) Zhang, W.; Tang, X.; Ma, H.; Sun, W.-H.; Janiak, C. *Eur. J. Inorg. Chem.* **2008**, 2830. (c) Neve, F.; Crispini, A. *Cryst. Growth Des.* **2001**, *1*, 287.
(23) Knutson, J. L.; Martin, J. D.; Mitzi, D. B. *Inorg. Chem.* **2005**, *44*, 4699.
(24) Borriello, I.; Cantele, G.; Ninno, D. *Phys. Rev. B* **2008**, *77*, 235214.